AFRL-RX-WP-JA-2014-0201

ANALYSIS OF TIME DEPENDENT ELECTRIC FIELD DEGRADATION IN ALGAN/GAN HEMTS (POSTPRINT)

Eric R. Heller
AFRL/RXAN

OCTOBER 2014
Interim Report

AIR FORCE RESEARCH LABORATORY
MATERIALS AND MANUFACTURING DIRECTORATE
WRIGHT-PATTERSON AIR FORCE BASE, OH 45433-7750
AIR FORCE MATERIEL COMMAND
UNITED STATES AIR FORCE

NOTICE AND SIGNATURE PAGE

Using Government drawings, specifications, or other data included in this document for any purpose other than Government procurement does not in any way obligate the U.S. Government. The fact that the Government formulated or supplied the drawings, specifications, or other data does not license the holder or any other person or corporation; or convey any rights or permission to manufacture, use, or sell any patented invention that may relate to them.

This report was cleared for public release by the USAF 88th Air Base Wing (88 ABW) Public Affairs Office (PAO) and is available to the general public, including foreign nationals.

Copies may be obtained from the Defense Technical Information Center (DTIC) (http://www.dtic.mil).

AFRL-RX-WP-JA-2014-0201 HAS BEEN REVIEWED AND IS APPROVED FOR PUBLICATION IN ACCORDANCE WITH ASSIGNED DISTRIBUTION STATEMENT.

//Signature//

ERIC R. HELLER
Nanoelectronic Materials Branch
Functional Materials Division

//Signature//

DIANA M. CARLIN, Chief
Nanoelectronic Materials Branch
Functional Materials Division

//Signature//

TIMOTHY J. BUNNING, Chief
Functional Materials Division
Materials and Manufacturing Directorate

This report is published in the interest of scientific and technical information exchange, and its publication does not constitute the Government's approval or disapproval of its ideas or findings.

REPORT DOCUMENTATION PAGE

Form Approved
OMB No. 074-0188

1. REPORT DATE (DD-MM-YYYY)	2. REPORT TYPE	3. DATES COVERED *(From – To)*
October 2014	Interim	29 January 2013 – 30 September 2014

4. TITLE AND SUBTITLE
ANALYSIS OF TIME DEPENDENT ELECTRIC FIELD DEGRADATION IN ALGAN/GAN HEMTS (POSTPRINT)

5a. CONTRACT NUMBER
FA8650-11-D-5401-0011

5b. GRANT NUMBER

5c. PROGRAM ELEMENT NUMBER
61102F

6. AUTHOR(S)
(see back)

5d. PROJECT NUMBER
3001

5e. TASK NUMBER

5f. WORK UNIT NUMBER
X0K9

7. PERFORMING ORGANIZATION NAME(S) AND ADDRESS(ES)
(see back)

8. PERFORMING ORGANIZATION REPORT NUMBER

9. SPONSORING / MONITORING AGENCY NAME(S) AND ADDRESS(ES)
Air Force Research Laboratory
Materials and Manufacturing Directorate
Wright Patterson Air Force Base, OH 45433-7750
Air Force Materiel Command
United States Air Force

10. SPONSOR/MONITOR'S ACRONYM(S)
AFRL/RXAN

11. SPONSOR/MONITOR'S REPORT NUMBER(S)
AFRL-RX-WP-JA-2014-0201

12. DISTRIBUTION / AVAILABILITY STATEMENT
Distribution A. Approved for public release; distribution unlimited. This report contains color.

13. SUPPLEMENTARY NOTES
PA Case Number: 88ABW-2014-0825; Clearance Date: 27 February 2014. Journal article published in IEEE Transactions On Electron Devices, Vol. 61, No. 9, September 2014. © 2014 IEEE. The U.S. Government is joint author of the work and has the right to use, modify, reproduce, release, perform, display or disclose the work. The final publication is available at 10.1109/TED.2014.2336248.

14. ABSTRACT
The authors report on an electrical and optical analysis of AlGaN/GaN HEMTs stressed under high electric field conditions into a state of permanent degradation, evidenced by an increase in OFF-state leakage current and a reduction in breakdown voltage. A method of stress testing AlGaN/GaN HEMTs to voltages close to breakdown while protecting the device from catastrophic failure is presented. Using this stress method, a detailed study was performed to observe device degradation that limits safe operation in the OFF-state. Electrical analysis reveals that quantitatively the Schottky properties of the gate diode are degraded by the stress and suggests a localized defect. An optical analysis confirms localized degradation via electroluminescence (EL) spots on the stressed side of the gate finger. It is shown that the dominant EL site in the degraded device may be observed prior to the application of stress. Finally, it is confirmed that the localized EL emission of the stressed device is the dominant gate leakage path via thermal imaging. These results suggest a method for identifying and understanding the failure mechanisms that limit the safe operating area of GaN HEMTs.

15. SUBJECT TERMS
aluminum gallium nitride, gallium nitride, HEMTs, semiconductor device reliability, transistors

16. SECURITY CLASSIFICATION OF:			17. LIMITATION OF ABSTRACT	18. NUMBER OF PAGES	19a. NAME OF RESPONSIBLE PERSON *(Monitor)*
a. REPORT	b. ABSTRACT	c. THIS PAGE			Eric R. Heller
Unclassified	Unclassified	Unclassified	SAR	11	19b. TELEPHONE NUBER *(include area code)* (937) 938-8746

Standard Form 298 (Rev. 2-89)
Prescribed by ANSI Std. Z39-18

REPORT DOCUMENTATION PAGE Cont'd

6. AUTHOR(S)

Eric R. Heller - Materials and Manufacturing Directorate, Air Force Research Laboratory, Functional Materials Division

Michael D. Hodge, Ramakrishna Vetury, and Jeffrey B. Shealy - Department of Electrical and Computer Engineering, University of North Carolina at Charlotte

7. PERFORMING ORGANIZATION NAME(S) AND ADDRESS(ES)

AFRL/RXAN
Air Force Research Laboratory
Materials and Manufacturing Directorate
Wright-Patterson Air Force Base, OH 45433-7750

Dept. of Electrical and Computer Engineering
University of North Carolina at Charlotte
890 Oval Drive
Raleigh NC 27606

Analysis of Time Dependent Electric Field Degradation in AlGaN/GaN HEMTs

Michael D. Hodge, Eric R. Heller, Ramakrishna Vetury, and Jeffrey B. Shealy

***Abstract*— The authors report on an electrical and optical analysis of AlGaN/GaN HEMTs stressed under high electric field conditions into a state of permanent degradation, evidenced by an increase in OFF-state leakage current and a reduction in breakdown voltage. A method of stress testing AlGaN/GaN HEMTs to voltages close to breakdown while protecting the device from catastrophic failure is presented. Using this stress method, a detailed study was performed to observe device degradation that limits safe operation in the OFF-state. Electrical analysis reveals that quantitatively the Schottky properties of the gate diode are degraded by the stress and suggests a localized defect. An optical analysis confirms localized degradation via electroluminescence (EL) spots on the stressed side of the gate finger. It is shown that the dominant EL site in the degraded device may be observed prior to the application of stress. Finally, it is confirmed that the localized EL emission of the stressed device is the dominant gate leakage path via thermal imaging. These results suggest a method for identifying and understanding the failure mechanisms that limit the safe operating area of GaN HEMTs.**

***Index Terms*— Aluminum gallium nitride, gallium nitride, HEMTs, semiconductor device reliability, transistors.**

I. Introduction

AlGaN/GaN HEMTs have made major strides in recent years toward achieving widespread adoption in a variety of high power and high frequency applications. A complete understanding of failure mechanisms that limit the safe operating area (SOA) of GaN devices provides the means of unlocking additional capability of GaN technology needed for many emergent applications of GaN devices in power electronics and RF switches, in addition to the RF power amplifiers.

Two main mechanisms have been proposed in literature limiting device lifetimes when exposed to low-power high electric field stress. Initial reports proposed the existence of a critical voltage that when exceeded, leads to the formation of a crack or pit in the crystal due to mechanical stress resulting from the inverse piezoelectric effect [1]–[6]. Since the publication of the inverse piezoelectric effect, many authors have reported that device degradation in the presence of high electric fields has a significant time dependence. This time dependence presents complications in a simple inverse piezoelectric effect driven model [7]–[11]. More recently, Marcon *et al*. [12] have postulated that the time-dependent degradation mechanism results from the formation of percolation paths that are created in the AlGaN barrier. This percolation mechanism is proposed to be similar to the mechanism observed in time-dependent dielectric breakdown of capacitors.

In this paper, a method of stress is proposed that allows a device to be stressed close to permanent breakdown, beyond the recommended safe operating limits of the process, without catastrophically destroying the device, so that it may be examined for root cause effects. This method was performed on devices fabricated using a commercially available and qualified AlGaN/GaN HEMT fabrication process [13]. The devices were then stressed close to catastrophic breakdown and characterized for parametric shifts due to stress. An electrical analysis of device characteristics over temperature is presented that points to degradation in the Schottky properties of the gate diode with stress. Furthermore, this analysis suggests that gate diode degradation is localized within the gate periphery and is the limiting aspect of device breakdown after stress. Also presented is an optical analysis as the device degrades with stress. This analysis confirms that the degradation to the device gate diode is localized due to the formation of a localized electroluminescence (EL) emission site when biased in the OFF-state after stress, in agreement with [9]. It is reported that EL emission is also present in the unstressed device at the site of OFF-state EL emission post stress, suggesting the possibility that weak areas along the gate finger may be observed prior to stress. Finally, it is confirmed that the localized EL emission site after stress corresponds to the region of increased gate leakage observed via thermal imaging.

II. Experiment

A. Device Details

The AlGaN/GaN HEMTs on SiC substrates in this work were grown by metal-organic chemical vapor deposition and fabricated using a process that was qualified for commercial production [13]. However, the device in this paper used an experimental layout that deviated from the qualified layout in two key areas. First, the gate-to-drain and gate-to-source contact spacing was minimized to create a device with the

Manuscript received April 3, 2014; accepted July 1, 2014. Date of publication July 25, 2014; date of current version August 19, 2014. This work was supported by the National Reconnaissance Office/Air Force Research Laboratory High Reliability Electronics Virtual Center. The review of this paper was arranged by Editor G. Ghione.

M. D. Hodge is with the Department of Electrical and Computer Engineering, University of North Carolina at Charlotte, Charlotte, NC 28223 USA, and also with RF Micro Devices, Charlotte, NC 28269 USA.

E. R. Heller is with the Materials and Manufacturing Directorate, Air Force Research Laboratory, Wright-Patterson Air Force Base, OH 45433 USA.

R. Vetury and J. B. Shealy are with RF Micro Devices, Charlotte, NC 28269 USA.

Color versions of one or more of the figures in this paper are available online at http://ieeexplore.ieee.org.

Digital Object Identifier 10.1109/TED.2014.2336248

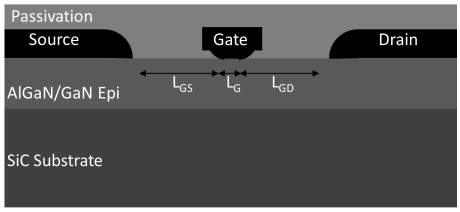

Fig. 1. AlGaN/GaN HEMT device cross section schematic with key dimensions labeled.

lowest breakdown voltage possible. This allowed the device to be stressed with a semiconductor parametric analyzer (SPA), capable of accurate measurement of leakage current during stress. Second, the source-connected field plate was removed in this layout so that optical analysis was feasible close to the edge of the gate contact. The devices had gate periphery (W_g) of 100 μm and a gate length (L_g) of 0.5 μm. The devices had the same gate-to-drain distance as the gate-to-source ($L_{gs} = L_{gd} = 1.3$ μm). A gate field plate was present as a consequence of processing the device T-gate. A representation of the channel cross section, with key dimensions labeled, is shown in Fig. 1. On resistance (R_{ON}) was measured as 1.9 Ωmm, drain current at $V_{gs} = 0$ V (I_{dss}) was 670 mA/mm, and max drain current (I_{dmax}) measured as 1050 mA/mm.

B. Electrical Stress

Studying semiconductor devices under high electric field conditions, especially near breakdown is challenging due to potential electrical over-stress (EOS) events that can lead to instantaneous catastrophic breakdown of the device. The extensive damage done to a device that experiences an EOS event prevents useful failure analysis. Therefore, to understand how devices fail under high electric field conditions it becomes imperative to develop a stress method that can degrade the part gradually so that the device may be studied at the conclusion of stress.

We explain the detail and motivation for the stress methodology as follows. The SPA was set to forced drain current mode. The drain voltage compliance was set at a desired value. In a constant forced current stress mode, the SPA continuously increases the applied drain voltage in an attempt to reach the set forced current. If the set value of the forced current is higher than the maximum leakage for a given device, the drain voltage reaches the compliance value before the drain leakage current attains the set value of forced current. Once drain voltage compliance is reached, the drain voltage is held fixed at the compliance limit by the instrument, effectively converting a constant current stress into a constant voltage stress. In this manner, the compliance voltage of the test becomes the set point of the voltage stress and is hence a key parameter of the test.

In the event of a device failure during stress, the maximum leakage current that can be forced through the device is limited to the constant current set value. If this set value is fixed slightly higher than the anticipated maximum leakage current of any particular device and then the drain compliance voltage is adjusted to the desired value, then the device can safely

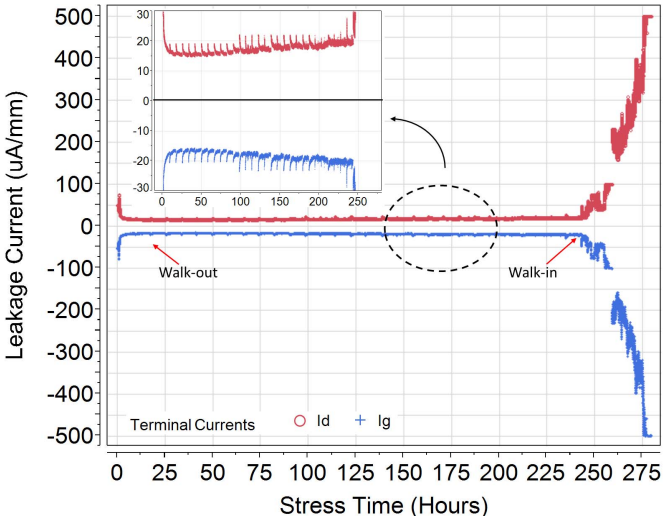

Fig. 2. Leakage currents measured at both the drain and gate terminals during stress. Both I_d and $|I_g|$ are nearly identical, indicating all leakage in the device is from gate to drain. Inset image shows the plot on a different scale to clearly show the recovery of leakage current at each characterization point.

be stressed at the desired voltage for an extended duration, without the risk of an EOS event. Controlling the drain in this way is superior to gate control in a similar fashion. This manner of control will protect the FET from catastrophic damage from either a sudden EOS failure due to an additional gate to drain current pathway or failure due to an additional source to drain current pathway. Control of the gate current only guards against an EOS event from drain to gate.

This technique was utilized in this paper to hold the device close to breakdown and therefore accelerate the degradation mechanism while at the same time preventing an EOS event. The gate bias was held at $V_{gs} = -10$ V and the induced drain bias was set to $V_{ds} = 120$ V. The device was stressed in 4–8 h intervals with a characterization step between each interval. The stress intervals were set to 8 h initially as minimal change was observed. Once degradation was observed intervals were shortened to collect more characterization data. The entire stress was conducted at room temperature.

After every stress interval, the device breakdown voltage was characterized via a three-terminal breakdown measurement. During this characterization, the bias conditions were, $V_{gs} = -10$ V and V_{ds} was swept from 0 to 125 V. The drain compliance was set to 100 μA/mm that stopped the test if this value was reached.

C. Electrical Degradation

A plot of the drain (I_d) and gate (I_g) terminal leakage currents during the stress of a representative device are shown in Fig. 2. Note that both gate and drain current are of similar magnitude, indicating the leakage current is dominated by drain to gate leakage, while drain to source leakage is negligible.

The leakage characteristics during stress behaved as reported in [11] using devices from this process. During the

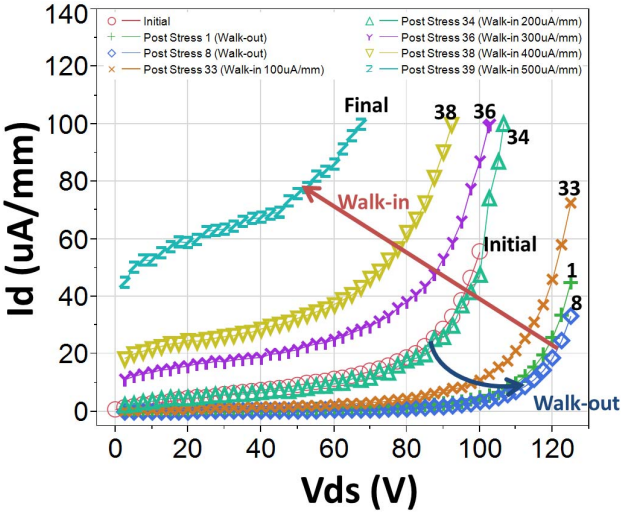

Fig. 3. Plot of three-terminal breakdown characterization that was performed at multiple intervals during the stress test of the device shown in Fig. 2. The numbering denotes the stress interval prior to the OFF-state characterization.

initial application of stress, the device undergoes walk-out during which the leakage current drops and breakdown voltage is enhanced. After a sufficient period of stress time, the device begins rapidly degrade and enters walk-in evidenced by an increase in leakage current and decrease in breakdown voltage.

The changes to the device during the walk-out phase are recoverable, as shown by the increase in leakage current after resuming stress at each stop/start point in the inset image of Fig. 2. This suggests the mechanism is due to surface trapping phenomenon.

During the walk-in phase, the changes to the device are irreversible suggesting that permanent damage has been caused to the device. This is observed in Fig. 2 after 245 h of stress time the leakage current of the device begins to rapidly increase. The electrical stress for all devices was concluded after the leakage current reached 500 μA/mm. This stop point was chosen to ensure that the sufficient degradation had occurred in the device so that subsequent analysis of the device would produce measurable results.

A plot of the breakdown voltage characterization is shown in Fig. 3. In this figure, only a subset of the characterizations are shown to illustrate the evolution in the breakdown with stress. During the walk-out portion, the breakdown voltage is enhanced and the leakage current decreased from the initial curve to first and eighth characterization points. The breakdown characterizations after the eighth point represent an increase in device leakage current and reduction in breakdown voltage that corresponds to walk-in.

III. Electrical Analysis

Electrical characterization of the stressed device at each stop point over temperature was analyzed for insight into the observed walk-in degradation. To study this phenomenon, a characterization of the gate diode was performed over temperature at three different time periods. The initial characterization was done prior to application of stress. The walk-out

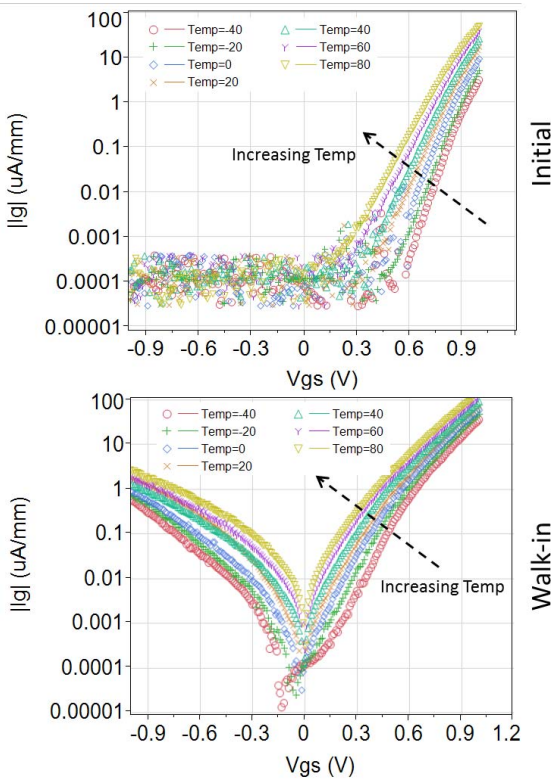

Fig. 4. Gate diode characterization with temperature shown at initial and walk-in. After walk-in the increase in reverse bias leakage current and shift in forward bias behavior suggests degradation of the Schottky diode properties.

characterization was performed immediately after the application of OFF-state stress for 1 h. The walk-in characterization was performed after the device had reached the targeted leakage current of 500 μA/mm. The characterization with temperature data was collected from -40 °C to 80 °C in 20 °C increments.

Two key observations are made from the diode characterization, between the initial characterization and after the onset of walk-in, shown in Fig. 4. First, in the forward direction, the shape of the diode curve has changed indicating a difference in ideality factor and effective barrier height. Second, in the reverse bias section of the curve, leakage current is shown to have increased three orders of magnitude from the initial values after walk-in.

To quantify the changes observed in the reverse diode characteristics, an attempt was made to fit the reverse leakage current to an established reverse Schottky diode leakage model. The reverse diode leakage in this paper has a temperature dependence that implies a trap assisted tunneling mechanism, as shown in [15]. An attempt was made to fit the reverse leakage data to the Poole–Frenkel model as presented in [15]. The data did not fit the model well but this is likely because the model assumes uniform leakage along the entire gate diode area. As will be shown in the optical analysis section, the leakage current from the degraded devices is localized within the gate periphery. Therefore, the leakage current at the localized defects may still be attributed to trap assisted tunneling mechanisms.

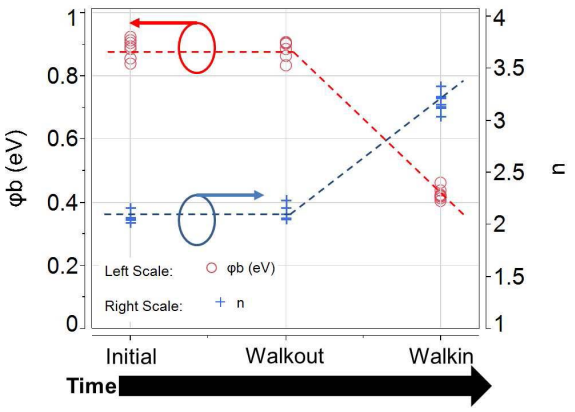

Fig. 5. Ideality factor and Schottky barrier height from gate diode characterization with temperature versus the device degradation state. The dotted lines are visual guides only.

To quantify the changes to the diode in the forward direction, both the ideality factor and the barrier height, were extracted from the data at each stress and temperature point. The ideality factor of the Schottky diode is given by the following:

$$n = \frac{q}{kT}\frac{\partial V_G}{\partial (ln I_G)}. \tag{1}$$

The barrier height of the Schottky diode was calculated using the following:

$$\phi_b = \frac{kT}{q} * \ln\frac{\mathrm{AA^*T^2}}{\mathrm{I_0}}. \tag{2}$$

A plot of the effective ideality factor and barrier height versus degradation stage is shown in Fig. 5. Since we propose the gate leakage post stress is not uniform along the gate periphery, these data are meant only to illustrate the average characteristics of the gate diode at each stage of degradation. In this figure, only the data from one device is shown, the multiple points at each stage are from the seven temperature points (−40 °C to 80 °C in 20 °C steps).

The data show minimal change to the diode properties from initial state to the walk-out state. However, the diode properties are significantly degraded from the walk-out stage to the walk-in stage. At room temperature, the ideality of the diode has degraded from 2.07 to 3.21 while the barrier height has lowered from 0.892 to 0.424 eV. The variance of the diode properties with temperature shows minimal change with degradation. During the initial characterization, the ideality of the diode varied by 0.14 and barrier height by 0.07 eV over temperature. At the walk-in stage, the range was 0.29 and 0.05 eV for both the ideality and barrier height, respectively.

In this section, it was shown that the degradation of the Schottky gate diode is responsible for the observed walk-in phenomena. When the gate diode is reverse biased, the leakage current increased and had a strong temperature dependence, suggesting a trap assisted tunneling mechanism. The forward bias properties of the diode were quantitatively shown to have degraded when stressed to the walk-in state.

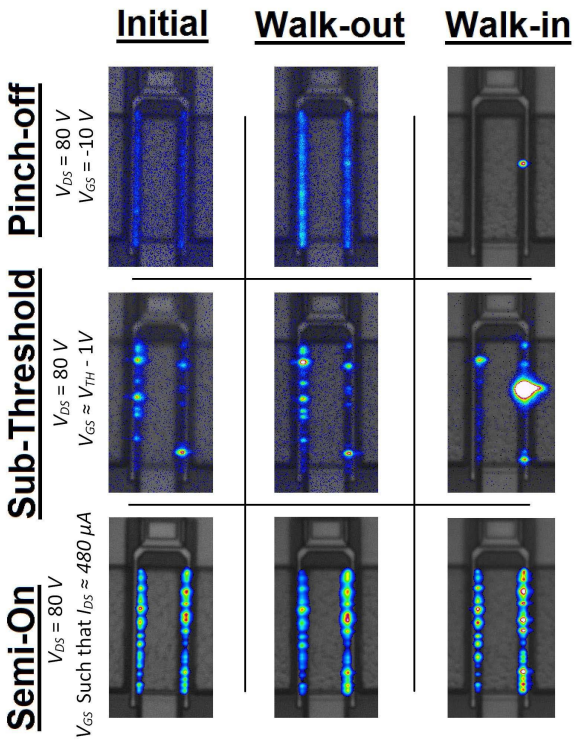

Fig. 6. EL mapping of a representative device in this paper with each column corresponding to a stage of stress after which the device was characterized. Each row corresponds to a different bias conditions.

IV. Optical Analysis

One of the challenges of time-dependent electric field degradation studies of AlGaN/GaN HEMTs has been the difficulty in capturing physical evidence. Unlike the inverse piezoelectric effect, that manifests as a crack or pit in regions of high electric field, studies involving time-dependent degradation have been unable to reveal a clear macroscopic defect.

A. Electroluminescence

EL is one method utilized to identify an area of interest along the periphery of a device. This is done by reverse biasing the device and searching for light emission [near-infrared (IR) and/or visible] along the gate finger, as shown in Fig. 6. Several publications have reported localized EL emission detected on devices stressed in the OFF-state and report a correlation of real time increases in leakage current during stress with the formation of local EL sites [8]– [10], [16], [17]. However, attempts to uncover physical evidence of crystallographic deformation at these emission sites had limited success [11], [12], [14]. The only crystal defect mentioned is the formation of surface pits described in [17]. It has been proposed in [12] that a leakage path is formed via percolation paths through the AlGaN barrier layer that are not physically observable.

In this paper, all six devices were characterized by EL in the walk-in state. Four of the devices were characterized at both walk-out and walk-in. Finally, two of the devices were characterized at all three stages of initial, walk-out, and walk-in. The general behavior was consistent in all devices.

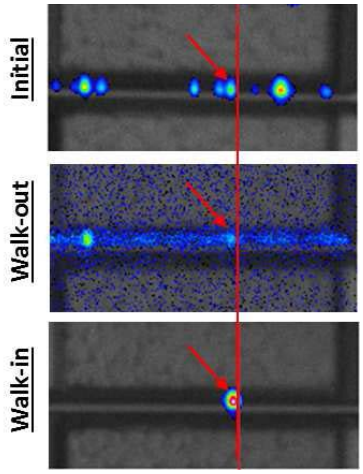

Fig. 7. Zoomed-in view of the EL images of the same device in Fig. 6. It is shown that the location that eventually becomes the dominant EL emission site after walk-in is also present in the initial and walk-out images.

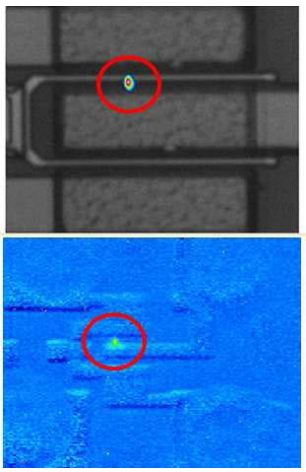

Fig. 8. Top: EL image of a device that has been stressed to walk-in with a localized emission site on the drain side of the top gate finger. Bottom: same device with a localized IR hotspot at the same location.

Fig. 6 shows the evolution of the EL across all three stages from one of the representative devices.

The bias conditions in Fig. 6 are full OFF-state ($V_{gs} = -10$ V and $V_{ds} = 80$ V), subthreshold ($V_{gs} = V_{th} - 1$ V$= -4.45$ V and $V_{ds} = 80$ V), and semi-ON ($I_{ds} = 480$ μA and $V_{ds} = 80$ V). All of the EL emission appear on the drain-side edge of the gate finger. Both the initial and walk-out EL characterizations look similar. In the semi-ON bias conditions EL may be observed, with varying degrees of intensity, along the entire gate finger. In the subthreshold condition, much of the light along the gate finger is extinguished but some EL emission sites persist that may indicate local variations of threshold voltage along the gate finger. After V_{gs} is biased well below V_{th}, all localized EL emissions sites are very low in intensity prior to walk-in.

In comparing the EL emission from initial and walk-out to the walk-in, some changes are observable in the device. Clear evidence of change is difficult to distinguish in the semi-ON state but a very bright EL emission site is visible in the subthreshold and deep pinch-off toward the center of the right-side gate finger in Fig. 6. In the subthreshold condition, the sparse EL emission is still present as was observed in the previous stages but now a dominant EL site is clearly present. The dominant EL site persists when the device is biased completely OFF after walk-in was observed.

Study of EL over a range of device states of operation is necessary to evaluate and understand localized emission along the gate finger, because in this work what will eventually become the dominant EL emission site is not observable at all bias conditions prior to walk-in degradation. Instead, other localized emission sites exist, that do not evolve into a significant leakage current path with stress. It is not clear at this time, the exact relationship between eventual degradation with OFF-state stress and the presence of these sites. It is worthwhile to note that localized emission does not necessarily indicate that site is a stress induced damaged section of the gate diode.

An effort is made in Fig. 7 to understand the evolution of EL emission at the localized site within the gate periphery that transforms into the dominant EL emission site after walk-in. Figure 7 shows that EL emission is present at what will eventually become the dominant EL emission site at both the initial and walk-out characterization. This suggests that localized EL sites observed prior to stress may indicate areas of the gate finger that are more susceptible to degradation with OFF-state stress.

Cross-sectional TEM images at the localized emission site of a device stressed to walk-in and a control unstressed part showed no clear evidence of a defect. The devices stressed to walk-in did not have surface cracking or pitting at the dominant EL emission site. Furthermore, material defects at the emission site, such as threading dislocations were not significantly different compared with the control site in both density and location of material defects with respect to the gate contact. No clear processing defects were evident in gate contact formation.

B. Thermal IR

The intensity of EL is affected by the localized current, the efficiency of emission of photons of a suitable energy to be detectable of that local current (which can vary by orders of magnitude), and the efficiency with which light can reach the detector (peak emission is likely under the gate field plate). Furthermore, because GaN and SiC are optically transparent and can channel light to other locations, is it not obvious that EL emission implies locally high leakage current.

To confirm the localized EL emission site was the actual site of the increase in leakage current during walk-in, a thermal IR measurement ($\lambda = 2$–5 μm) was made on the same device. IR measurements of devices biased into the OFF-state are challenging since power dissipation needed to achieve a measurable signal is difficult to obtain. In the OFF-state, very little current is conducted in the device, typically on the order of 10 s of microamperes for a degraded device. In addition, the max voltage of the device is limited by the breakdown that has degraded during the walk-in process. To generate a measurable IR result in this work, the test conditions were $V_{gs} = -10$ V, $V_{ds} = 110$ V, $P_{diss} = 3.84$ mW, and $T_{base} = 41$ °C.

The observed thermal IR signature is shown at the bottom of Fig. 8. Both the EL and IR emission sites are spatially close enough to be considered the same location along the gate finger. This observation was confirmed for two other devices in this study.

V. Conclusion

The work presented in this paper provides a method of stressing AlGaN/GaN HEMTs close to catastrophic breakdown while at the same time avoiding an EOS event. This method allows for studying the effects of high electric field applied to a device biased in the OFF-state. Utilizing this stress method, several key observations were made that suggests this technique is valuable for assessing the SOA in the OFF-state. An analysis is presented of both electrical and optical signatures in commercially available AlGaN/GaN HEMTs stressed close to catastrophic breakdown, beyond the safe operating conditions. The changes to the device observed during stress consist of breakdown voltage walk-out and eventually walk-in that is linked to an irrecoverable degradation mechanism. The increased leakage current measured in the device after stress is due to a dominant path from the drain to gate terminal of the device, suggesting a degradation in the Schottky barrier properties of the gate. Electrical and optical analysis supports the hypothesis that leakage current is localized to specific sites along the gate finger within the total gate periphery of the device.

In the presented electrical analysis, we have demonstrated evidence of Schottky diode degradation. First, it was shown that the reverse leakage has a significant temperature dependence and is consistent with trap-assisted tunneling mechanisms reported in literature. Second, the forward diode properties were quantitatively analyzed to show a reduction in Schottky barrier height and ideality.

Optical analysis was performed on the AlGaN/GaN HEMTs, prior to stress and after the walk-out and walk-in conditions. First, it was discovered that localized emission along the gate finger is present when biased above threshold but this emission nearly vanished when the device was biased well below the threshold voltage prior to degradation. After the observed degradation in the walk-in state, a localized EL emission site was revealed in the OFF-state that is consistent with [8]–[10], [16], and [17]. Second, to the best of the author's knowledge, this is the first time it has been shown that a localized EL emission site was present prior to stress, at the area of the gate finger that would eventually evolve into the dominant EL site after permanent degradation. This indicates that localized areas along the gate finger may be more susceptible to degradation as processed prior to stress. Third, for the first time, it was confirmed that the localized EL emission observed in the OFF-state after degradation corresponds to the region of the gate finger that is the source of reverse leakage current via IR imaging.

Cross-sectional images of the devices at the dominant EL emission site did not produce any obvious defects when compared with control cross sections on an unstressed device. There was no evidence of surface cracking or pitting as observed in literature attributing failure to the inverse piezoelectric effect. No material or processing defects were obvious in the cross-sectional images when comparing stressed devices to each other and to a control unstressed device. The absence of a physically observable defect suggests that the failure mechanism is related to time-dependent dielectric breakdown and formation of percolation paths as was suggested in [12]. In summary, these observations together with the method of stress testing described in this paper, suggests a methodology for identifying and understanding the failure mechanisms that limit the SOA of GaN HEMTs.

References

[1] J. Joh and J. A. Del Alamo, "Mechanisms for electrical degradation of GaN high-electron mobility transistors," in *Proc. Electron Devices Meeting (IEDM)*, Dec. 2006, pp. 1–4.

[2] J. Joh and J. A. Del Alamo, "Critical voltage for electrical degradation of GaN high-electron mobility transistors," *Electron Device Lett.*, vol. 29, no. 4, pp. 287–289, Apr. 2008.

[3] J. A. Del Alamo and J. Joh, "GaN HEMT reliability," *Microelectron. Rel.*, vol. 49, nos. 9–11, pp. 1200–1206, Sep. 2009.

[4] P. Makaram, J. Joh, J. A. Del Alamo, T. Palacios, and C. V. Thompson, "Evolution of structural defects associated with electrical degradation in AlGaN/GaN high electron mobility transistors," *Appl. Phys. Lett.*, vol. 96, no. 23, p. 233509, Jun. 2010.

[5] S. Demirtas and J. A. Del Alamo, "Critical voltage for electrical reliability of GaN high electron mobility transistors on Si substrate," in *Rel. Compound Semicond. Dig. (ROCS)*, Oct. 2009, pp. 53–56.

[6] J. L. Jimenez and U. Chowdhury, "X-band GaN FET reliability," in *Proc. IEEE Int. Rel. Phys. Symp. (IRPS)*, May 2008, pp. 429–435.

[7] D. Marcon *et al.*, "Reliability of AlGaN/GaN HEMTs: Permanent leakage current increase and output current drop," *Microelectron. Rel.*, vol. 52, nos. 9–10, pp. 2188–2193, Sep. 2012.

[8] G. Meneghesso *et al.*, "Reliability of GaN high electron mobility transistors: State of the art and perspectives," *IEEE Trans. Device Mater. Rel.*, vol. 8, no. 2, pp. 332–342, Jun. 2008.

[9] E. Zanoni *et al.*, "Localized damage in AlGaN/GaN HEMTs induced by reverse-bias testing," *IEEE Electron Device Lett.*, vol. 30, no. 5, pp. 427–429, May 2009.

[10] M. Meneghini *et al.*, "Time-dependent degradation of AlGaN/GaN high electron mobility transistors under reverse bias," *Appl. Phys. Lett.*, vol. 100, no. 3, pp. 033505-1–033505-3, Jan. 2012.

[11] M. D. Hodge, R. Vetury, and J. B. Shealy, "Fundamental failure mechanisms limiting maximum voltage operation in AlGaN/GaN HEMTs," in *Proc. IEEE Int. Rel. Phys. Symp. (IRPS)*, Apr. 2012, pp. 3D.2.1–3D.2.6.

[12] D. Marcon *et al.*, "Reliability analysis of permanent degradations on AlGaN/GaN HEMTs," *IEEE Trans. Electron Devices*, vol. 60, no. 10, pp. 3132–3141, Oct. 2013.

[13] RF Micro Devices. (2013). *GaN Open Foundry Services*. [Online]. Available: http://rfmd.com/openfoundry/GaNFoundry.aspx

[14] B. D. Christiansen *et al.*, "Reliability testing of AlGaN/GaN HEMTs under multiple stressors," in *Proc. IEEE Int. Rel. Phys. Symp. (IRPS)*, Apr. 2011, pp. CD.2.1–CD.2.5.

[15] H. Zhang, E. J. Miller, and E. T. Yu, "Analysis of leakage current mechanisms in Schottky contacts to GaN and $Al_{0.25}Ga_{0.75}N$/GaN grown by molecular-beam epitaxy," *J. Appl. Phys.*, vol. 99, no. 2, pp. 023703-1–023703-5, Jan. 2006.

[16] C. Hodges *et al.*, "Optical investigation of degradation mechanisms in AlGaN/GaN high electron mobility transistors: Generation of non-radiative recombination centers," *Appl. Phys. Lett.*, vol. 100, no. 11, pp. 112106-1–112106-4, Feb. 2012.

[17] M. Montes Bajo, C. Hodges, M. J. Uren, and M. Kuball, "On the link between electroluminescence, gate current leakage, and surface defects in AlGaN/GaN high electron mobility transistors upon off-state stress," *Appl. Phys. Lett.*, vol. 101, no. 3, pp. 033508-1–033508-4, Jul. 2012.

Michael D. Hodge received the B.S. degree in electrical and computer engineering from North Carolina State University, Raleigh, NC, USA, in 2004, and the M.S. degree in electrical engineering from the University of North Carolina at Charlotte, Charlotte, NC, USA, in 2007, where he is currently pursuing the Ph.D. degree.

He has been with RF Micro Devices, Charlotte, for the last seven years.

Eric R. Heller received the Ph.D. degree in physics from the Ohio State University, Columbus, OH, USA, in 2003.

His current research interests include physics-based modeling of electrical, thermal, and stress effects in widebandgap devices, with a current focus on modeling, characterization, and failure analysis to understand initial performance and long-term degradation of GaN high-electron mobility transistors.

Ramakrishna Vetury received the bachelor's degree in electronics and communication engineering from IIT Madras, Chennai, India, and the M.S. and Ph.D. degrees in electrical engineering from the University of California at Santa Barbara, Santa Barbara, CA, USA.

He is with the Power Broadband Business Unit, RFMD, Charlotte, NC, USA, as an Engineering Manager of RFMD's Open Foundry.

Jeffrey B. Shealy received the M.B.A. degree from Wake Forest University, Winston-Salem, NC, USA, and the Ph.D. degree in electrical engineering from the University of California at Santa Barbara, Santa Barbara, CA, USA.

He is the General Manager of the Defense and Power Business Unit with RFMD, Charlotte, NC, USA.

Dr. Shealy is a member of the IEEE Electron Device Society.